Nanoscale

PAPER

View Article Online
View Journal | View Issue

Cite this: *Nanoscale*, 2014, **6**, 8107

Platinum nanocatalysts loaded on graphene oxide-dispersed carbon nanotubes with greatly enhanced peroxidase-like catalysis and electrocatalysis activities†

Hua Wang,*[a] Shuai Li,[a] Yanmei Si,[a] Ning Zhang,[a] Zongzhao Sun,[a] Hong Wu[b] and Yuehe Lin*[bc]

A powerful enzymatic mimetic has been fabricated by employing graphene oxide (GO) nanocolloids to disperse conductive carbon supports of hydrophobic carbon nanotubes (CNTs) before and after the loading of Pt nanocatalysts. The resulting GOCNT–Pt nanocomposites could present improved aqueous dispersion stability and Pt spatial distribution. Unexpectedly, they could show greatly enhanced peroxidase-like catalysis and electrocatalysis activities in water, as evidenced in the colorimetric and electrochemical investigations in comparison to some inorganic nanocatalysts commonly used. Moreover, it is found that the new enzyme mimetics could exhibit peroxidase-like catalysis activity comparable to natural enzymes; yet, they might circumvent some of their inherent problems in terms of catalysis efficiency, electron transfer, environmental stability, and cost effectiveness. Also, sandwiched electrochemical immunoassays have been successfully conducted using GOCNT–Pt as enzymatic tags. Such a fabrication avenue of noble metal nanocatalysts loaded on well-dispersed conductive carbon supports should be tailored for the design of different enzyme mimics promising the extensive catalysis applications in environmental, medical, industrial, and particularly aqueous biosensing fields.

Received 21st February 2014
Accepted 30th April 2014

DOI: 10.1039/c4nr00983e

www.rsc.org/nanoscale

1. Introduction

Enzymes have been widely used in industrial, environmental, and medical fields, such as the catalytic oxidation of various toxic organic species in wastewater treatments,[1,2] and enzyme-based sensing of numerous biomarkers of clinical and environmental importance.[3,4] Natural enzymes, however, can suffer from some serious disadvantages regarding easy thermal denaturation, catalytic activity inhibition, and protease digestion of enzymes. An additional challenge can be associated with the enzymatic protein shells that can electrically insulate the redox center of natural peroxidases.[4] Alternatively, considerable efforts have been contributed to the studies on artificial enzyme mimics,[5,6] mostly known as peroxidase mimics including haematin,[7] hemin,[8] cytochrome,[9] and other organic and inorganic mimics.[10–12] However, they may somewhat achieve limited success in terms of catalysis efficiency, aqueous dispersion, and conductivity especially for electrochemical applications.

Materials on a nanoscale can present unique physical and chemical properties different from what they exhibit on a macroscale. As the most known one, noble metals like platinum (Pt) may be chemically inert at bulk scales but can serve as catalysts at nanoscales. Most known are Pt nanoparticles (Pt Nanos) that can present enzyme-like catalysis activity for sensing H_2O_2 or for scavenging superoxide free radicals.[13,14] In practical catalysis applications, however, the catalysis performances of Pt Nanos are generally limited by their low dispersive stability and partly blocked electron-transfer pathways or catalysis-active sites by the surface modifiers necessary for stabilizing high-energy surfaces of Pt nanomaterials in the synthesis procedure. Moreover, carbon nanotubes (CNTs) as an important group of conductive nanomaterials have received considerable interest for applications.[15,16] Due to their high surface area, mechanical strength and excellent electric conductivity, CNTs have been used as conductive electrode materials and catalyst supports in constructing fuel cells,[17–19] or as adsorption matrices and electron mediators for electrochemical sensor designs.[20–23] Particularly, CNTs are widely employed to support Pt nanocatalysts for heterogeneous

[a]*Shandong Province Key Laboratory of Life-Organic Analysis, School of Chemistry and Chemical Engineering, Qufu Normal University, Qufu City 273165, P. R. China. E-mail: huawangqfnu@126.com*

[b]*Pacific Norwest National Laboratory, Richland, WA 99352, USA. E-mail: yuehe.lin@pnnl.gov; Fax: +1 509 371 6242; Tel: +1 509 371 6241*

[c]*School of Mechanical and Materials Engineering, Washington State University, Pullman, WA 99164, USA*

† Electronic supplementary information (ESI) available: The catalysis mechanism, catalytic dynamic parameters, the interferent effects on H_2O_2 detections, investigations of time-dependent dispersion stabilities, double-reciprocal plots of catalysis activities, and electrocatalysis comparison between GOCNT–Pt nanocomposites and HRP. See DOI: 10.1039/c4nr00983e

electrocatalysis in fuel cells.[17,18,24] They have also been combined to fabricate the electrochemical platforms or load various enzymes to facilitate the electrocatalysis detection of glucose and/or H_2O_2 at a low potential.[25–27] Unfortunately, few investigations have been systematically conducted on the potential of CNT-supported Pt Nanos with peroxidase-like catalysis activity.

Moreover, most of the catalysis reactions with enzymes or their mimics are carried out in an aqueous system. The aqueous catalysis performances and the large-scale catalysis applications of CNT-supported Pt nanocatalysts, however, may be challenged by the poor aqueous dispersion of hydrophobic carbon supports and unfavorable distribution density of Pt nanocatalysts loaded generally by high thermal treatments. Therefore, increasing attention has been drawn to the improvement of the spatial distribution and dispersion stability of CNT supports in water, mostly known as the oxidation treatment[28] and surfactant addition.[29] Gracefully successful as these studies are, such a dispersion (or distribution) problem of CNT supports (or Pt nanocatalysts) remains far from well solved to date. Recent years have witnessed the rapid development of another amazing carbon material of graphene in the modern materials science and biotechnology.[12,30–33] Graphene has been used to attach Pt Nanos but to achieve only enhanced electrocatalytic activities,[34,35] while graphene oxide (GO) nanosheets might exhibit peroxidase-like catalysis.[12] Particularly, GO nanocolloids may serve as a wonderful "surfactant" for CNTs to create a stable dispersion of nanocolloids in water,[31–33] because they are amphiphilic with an edge-to-center distribution of hydrophilic and hydrophobic domains.[31]

In the present work, a new enzyme mimic has been fabricated by using GO nanocolloids to well disperse CNT supports before and after loading Pt Nanos. Unexpectedly, the resulting GOCNT–Pt nanocomposites could display high aqueous dispersion and desirable distribution density of nanocatalysts, and especially greatly enhanced peroxidase-like catalysis and electrocatalysis activities. To the best of our knowledge, this finding was reported and systemically studied for the first time. The powerful catalysis performances of GOCNT–Pt nanocomposites, here, were characterized by colorimetric H_2O_2 sensing and direct H_2O_2 electrochemistry, in comparison to CNT-and GO-supported Pt Nanos and natural protein enzyme commonly used, including the practical application as enzymatic labels for the sandwiched electrochemical immunoassays.

2. Results and discussion

2.1. Synthesis and characterization of GOCNT–Pt nanocomposites

The GOCNT–Pt nanocomposites have been fabricated by using the impregnation method. GO nanocolloids were first employed to well disperse CNTs to form the stable GOCNT suspension. Then, Pt precursors were physically adsorbed onto the GOCNTs followed by thermal treatment under an H_2 environment, achieving GOCNT–Pt nanocomposites with 20 wt% Pt redispersed in GO nanocolloids. Fig. 1 shows the topological structures and dispersions of the as-prepared GOCNT–Pt nanocomposites characterized by a transmission electron microscope (TEM), in comparison to the CNT–Pt nanocomposites fabricated

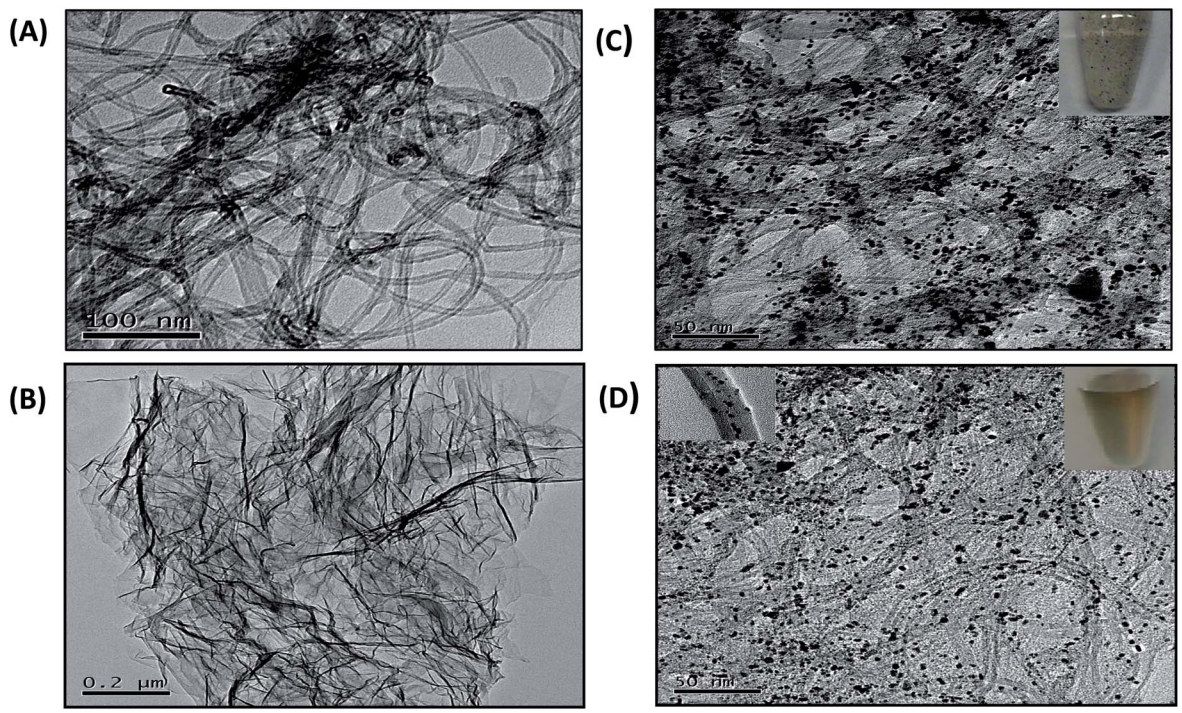

Fig. 1 Typical TEM images of (A) CNTs, (B) GO, (C) CNT–Pt nanocomposites (inset: the photograph of suspension solution (right top)), and (D) GOCNT–Pt nanocomposites in GO nanocolloids (inset: the amplified part of GOCNT–Pt (left top) and the photograph of suspension solution (right top)).

accordingly without GO nanosheets. One can note that Pt Nanos could be well loaded onto the pristine CNT (Fig. 1A) and the GO nanosheet (Fig. 1B) dispersed ones to yield CNT–Pt (Fig. 1C) and GOCNT–Pt (Fig. 1D), respectively. As manifested in the TEM images, however, the GOCNT–Pt could enable better spatial distribution density of Pt nanocatalysts on the carbon supports than the CNT–Pt. Also, the inseted photographs of their suspension solution show that GOCNT–Pt nanocomposites showed higher dispersion and stability than CNT–Pt ones that seemed to be partly coagulated and stacked in water. Furthermore, comparable investigations of dispersion stabilities were carried out for the GOCNT–Pt and CNT–Pt nanocomposites by using dynamic light scattering (DLS) at a 90° scattering angle (Fig. S1A, ESI†). It is found that the hydrodynamic diameters of the GOCNT–Pt and CNT–Pt concentrated at ~175 nm and ~188 nm, respectively, showing the difference in size distribution of GO-dispersed nanotube bundles in water. Moreover, the time-dependent dispersion of the GOCNT–Pt and CNT–Pt suspensions was evaluated by DLS and UV/vis spectrometry, where the sample supernatants were taken out and monitored at different time intervals (Fig. S1B, ESI†). As can be seen from the DLS intensities and optical absorbance values (250 nm) over time, the GOCNT–Pt could display much higher dispersion stability than the CNT–Pt, confirming the vital role of the GO "surfactant" in dispersing carbon supported Pt nanocomposites. In addition, the high magnification view of the GOCNT–Pt (the inset of Fig. 1D) clearly verifies that a single CNT bundle was decorated with Pt Nanos of 3.0 ± 0.5 nm with high dispersion and favorable distribution density. Herein, high dispersion of Pt nanocatalysts may help to improve their electrocatalytic

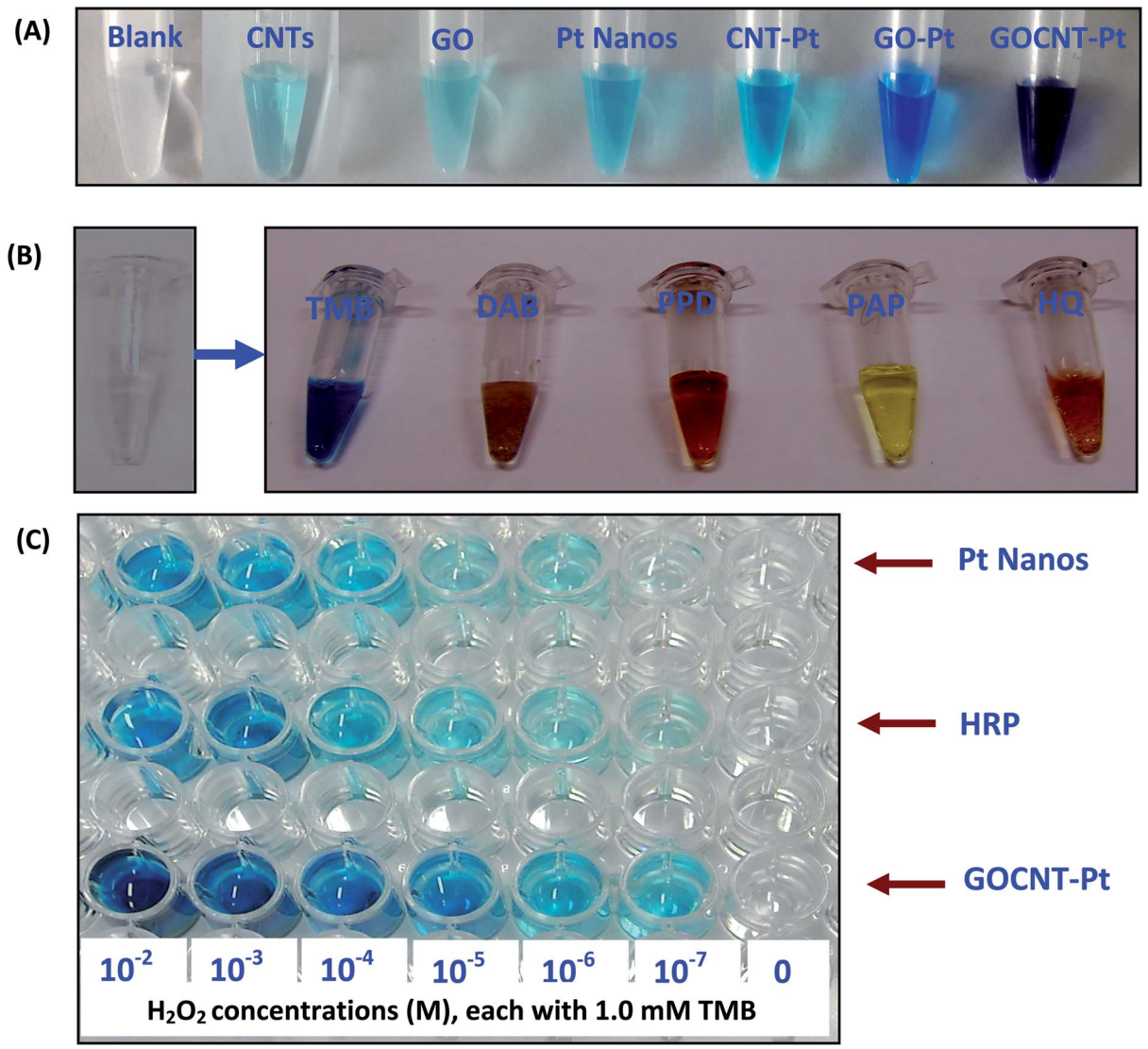

Fig. 2 Colorimetric investigations of peroxidase-like catalysis activities of GOCNT–Pt nanocomposites. (A) Comparison of catalytic redox reactions for the TMB-H_2O_2 substrate among CNTs, GOs, Pt Nanos, and the nanocomposites of GO–Pt, CNT–Pt, and GOCNT–Pt consisting of 0.05 mg mL^{-1} CNT or GO and/or 0.01 mg mL^{-1} Pt Nanos. (B) Catalytic oxidization of various organic substrates (1.0 mM) of TMB, DAB, PPD, AP and HQ using 0.05 mg mL^{-1} GOCNT–Pt nanocomposites with 4.0 mM H_2O_2. (C) Comparison of colorimetric H_2O_2 detection results among Pt Nanos, HRP, and GOCNT–Pt nanocomposites using 1.0 mM TMB and different H_2O_2 concentrations.

activities as recognized in fuel cell technologies.[36–38] Better mass transports of electrons and reactants also enable rapid electron shuttling and easy access of the reactants to their catalysis-active sites.[17] The synergetic effects of well dispersed carbon supports of high conductivity and Pt Nanos of intrinsic catalysis activity were thereby expected to facilitate both enhanced peroxidase-like catalysis and electrocatalysis of GOCNT–Pt nanocomposites.

2.2. Colorimetric investigations of peroxidase-like catalysis activities of GOCNT–Pt nanocomposites

The peroxidase-like catalysis activities of GOCNT–Pt nanocomposites were investigated by colorimetric tests with the 3,3′,5,5′-tetramethylbenzidine (TMB)–H_2O_2 substrate (Fig. 2A).

Herein, CNTs, GOs, Pt Nanos, CNT–Pt, and GO–Pt nanocomposites with the same carbon and/or Pt concentrations were utilized for comparison. It was observed that the GOCNT–Pt could catalyze H_2O_2-induced oxidization of TMB to yield a visible deep blue color within 15 min, resulting in color density much higher than those obtained for the Pt Nanos, CNT–Pt, and GO–Pt. Herein, GOs and CNTs might present a slight catalysis behavior to the TMB-H_2O_2 substrate, which might be comparably neglected. The results indicate that GOCNT–Pt nanocomposites could exhibit greatly enhanced peroxidase-like catalysis activity in contrast to the component materials, of which the supported Pt Nanos should be mainly responsible for the catalysis event.

Furthermore, the enzymatic catalysis capabilities of GOCNT–Pt nanocomposites were examined for the H_2O_2-induced oxidization of several peroxidase substrates, including 3,3′-diaminobenzidine (DAB), *p*-phenylenediamine (PPD), *p*-aminophenol (PAP), hydroquinone (HQ), and TMB. Fig. 2B illustrates the typical photographs of the colorful products of reactions. For example, the DAB solution changed to a brown color with a little of the resultant precipitate in catalysis reactions, and the PPD solution became a deep orange color. It is thereby believed that the GOCNT–Pt nanocomposites can show strong enzyme-catalytic behavior toward typical peroxidase substrates, indicating that they can be harnessed for catalytic degradation of toxic organic species so as to reduce their toxicity in the environment.

Moreover, colorimetric detections of H_2O_2 were performed by using the GOCNT–Pt nanocomposites, when compared to Pt Nanos and natural enzymes of horseradish peroxidase (HRP), which are commonly used (Fig. 2C). One can find that the color densities of the reaction products for both GOCNT–Pt nanocomposites and HRP can depend proportionally on H_2O_2 concentrations ranging from 10^{-7} to 10^{-2} M, which is much more sensitive than the H_2O_2 detection using Pt Nanos. Moreover, the peroxidase-like activities of GOCNT–Pt nanocomposites were characterized by the kinetic parameters, in comparison to GO–Pt and CNT–Pt, including documented HRP.[11] Typical Michaelis–Menten curves were plotted accordingly (Fig. S2, ESI†). With the Lineweaver–Burk equation, the Michaelis constant (K_m) and the maximal reaction velocity (V_{max}) were obtained and shown in Table S1, ESI.† The apparent K_m value of the GOCNT–Pt (1.82 mM) with the H_2O_2 substrate is lower than those of GO–Pt (4.24 mM), CNT–Pt (6.24 mM), and HRP (3.7 mM) reported elsewhere,[11] so is the apparent K_m of the GOCNT–Pt (0.075 mM) with the TMB substrate. The data suggest that the GOCNT–Pt could present a higher affinity for H_2O_2 and TMB. Therefore, the as-developed inorganic nanocatalysts can present catalysis performances comparable to natural peroxidase; yet, they may circumvent some inherent problems of natural enzymes.

Although many possible catalysis mechanisms have been proposed for Pt-catalytic H_2O_2 decomposition, the radical chain mechanism is herein assumed with the initiation reaction of OH-radical production catalyzed by Pt Nanos of a zero valence.[39,40] Herein, the proposed mechanism is detailed in Scheme S1, ESI.† Pt Nanos on carbon supports were thought to catalytically break the oxygen–oxygen bond of H_2O_2 to give OH radicals, which were stabilized at the surface of Pt Nanos.[39] The resulting OH radicals would further react with TMB to yield the blue reaction products. Obviously, GOCNT-supported Pt nanocatalysts might also benefit from GOCNT-enhanced electron-transferring ability and improved surface for easier access to the substrates, thus facilitating the stronger catalysis performances. In addition, colorimetric investigation of oxidase-like activity of GOCNT–Pt nanocomposites was performed using TMB in the presence and absence of oxygen (data not shown). Also, they could catalyze the TMB oxidization to yield blue products in the presence of dissolved oxygen serving as the electron acceptor, showing the great potential of oxidase-like functions of nanocatalysts.

2.3. Electrochemical investigations of electrocatalysis activities of GOCNT–Pt nanocomposites

The electrocatalysis characteristics of the GOCNT–Pt nanocomposites were investigated using H_2O_2 in the presence of TMB, taking the component materials of CNTs and Pt Nanos, CNT–Pt, and GO–Pt nanocomposites for comparison (Fig. 3).

Fig. 3A describes the typical voltammograms for detecting 2.0 mM H_2O_2. A well-defined pair of quasi-reversible redox peaks was obtained for the GOCNT–Pt electrode, with the oxidization and reduction potentials peaking at ~+ 0.11 V and ~+ 0.021 V, respectively. Notably, the redox currents for the GOCNT–Pt electrode are much higher than those of electrodes modified with Pt Nanos, CNT–Pt, and GO–Pt, although they might share the close peaking potentials presumably due to the existence of Pt Nano catalysts. By comparison, the CNT-modified electrode exhibited a more positive shift of the redox peak potentials in addition to significantly low current signals. More importantly, the GOCNT–Pt electrode could allow the electrochemical detection of H_2O_2 at a low potential, with voltammetric responses well proportional to H_2O_2 concentrations (Fig. 3B). Accordingly, the GOCNT–Pt catalysts can possess high electrocatalysis towards H_2O_2 reduction and organic substrate oxidation.

The direct electroanalysis to H_2O_2 using the GOCNT–Pt modified electrode was also tested, in comparison with the CNTs, Pt Nanos, CNT–Pt, and GO–Pt modified electrodes. Fig. 4A depicts the typical voltammograms at different

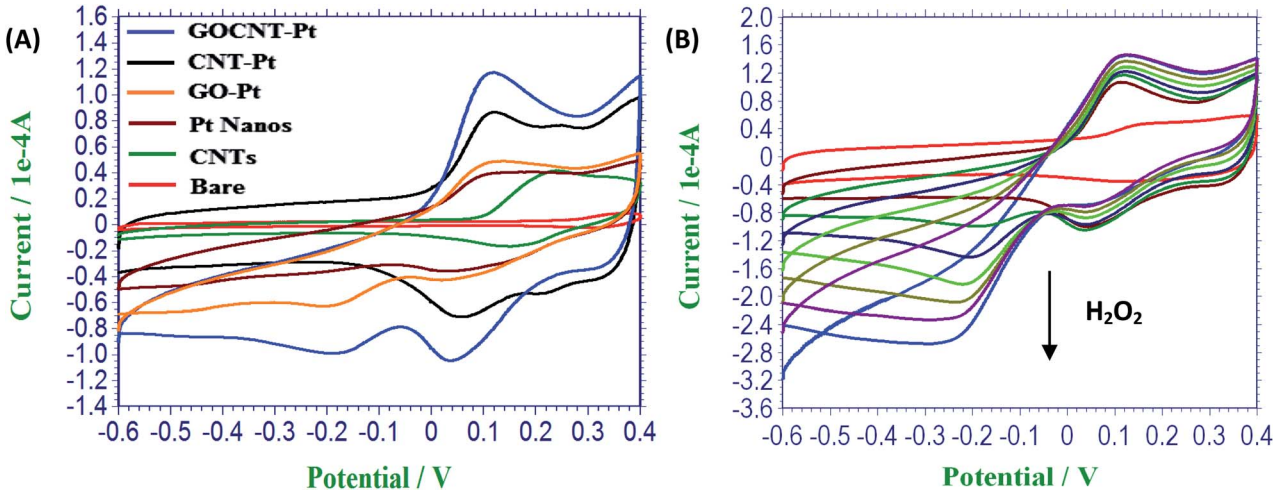

Fig. 3 Electrochemical response to H_2O_2 in the presence of TMB. (A) Comparison of typical voltammograms among the electrodes coated with bare, CNTs, Pt Nanos, GO–Pt, CNT–Pt, and GOCNT–Pt nanocomposites in the PBS solutions containing 2.0 mM H_2O_2 and 0.4 mM TMB, scanning from − 0.6 to + 0.4 V at a scan rate of 0.10 V s^{-1}. (B) Voltammograms at the GOCNT–Pt electrode for successive addition of 1.0 mM H_2O_2 in the presence of 0.4 mM TMB (red line for blank).

electrodes for the direct H_2O_2 electrochemistry. As expected, a great difference in voltammetric responses is obtained among these electrodes in the absence of an electronic mediator. The GOCNT–Pt modified electrode displayed the largest redox response to H_2O_2, which is ~10 times larger than that of the CNT modified electrodes commonly used. Particularly, a sharp H_2O_2 reduction peak was witnessed for the GOCNT–Pt electrode at ~−0.18 V when detecting 2.0 mM H_2O_2. In contrast, the potential peaks of other electrodes are much more negative, for example, it could peak at ~−0.45 V for the CNT-modified one. Fig. 4B manifests the voltammetric characteristics of the GOCNT–Pt electrode with direct responses to successive additions of H_2O_2, where the H_2O_2 reduction currents can increase proportionally with H_2O_2 levels.

In addition, the comparison of electrocatalysis capacity with the natural enzyme (*i.e.*, HRP) was also conducted. The electrode modified with GOCNT–Pt nanocomposites was evaluated in parallel with the electrode modified with pure HRP and CNT-loaded HRP (CNT-HRP), where H_2O_2 was detected in the presence and absence of the TMB mediator (Fig. S3A and B, ESI†). Again, much higher current responses and better redox peaks were obtained for the GOCNT–Pt electrode. The evidence indicates that the GOCNT–Pt might possess higher electron-transferring and electrocatalysis abilities than the natural enzyme, in

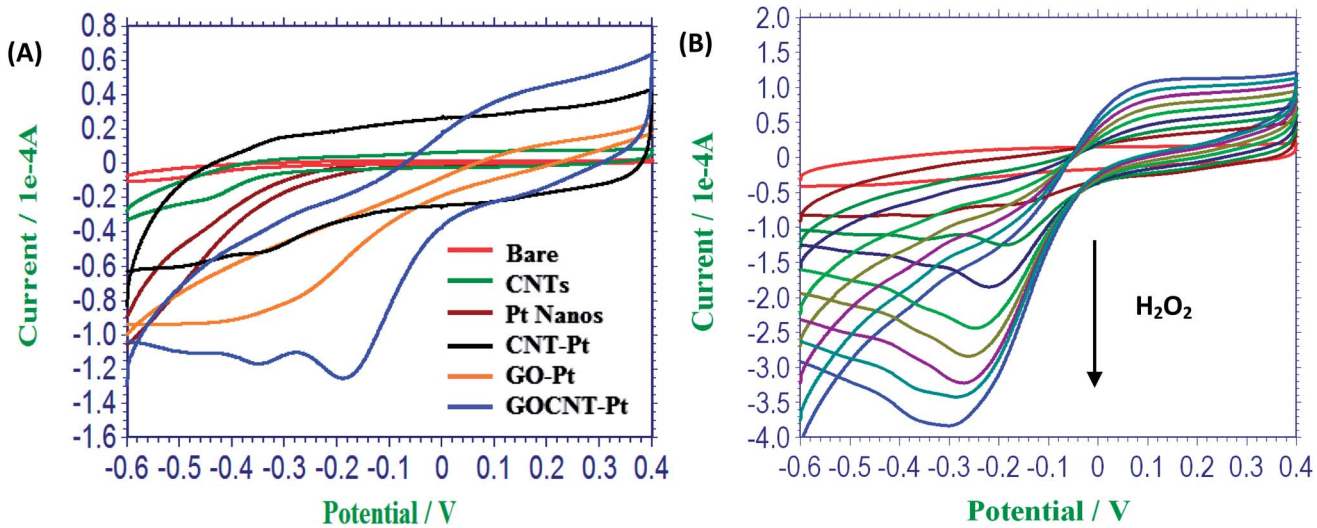

Fig. 4 Direct electrochemical responses to H_2O_2. (A) Comparison of typical voltammograms (the first scanning circle) among the electrodes modified with bare, CNTs, Pt Nanos, CNT–Pt, GO–Pt, and GOCNT–Pt nanocomposites separately in the PBS buffer containing 2.0 mM H_2O_2 under the same scanning conditions as in Fig. 3; (B) voltammograms of direct responses of the GOCNT–Pt electrode to successive addition of H_2O_2 at a step of 1.0 mM (red line for 0.0 mM H_2O_2).

electrochemical H_2O_2 reduction, even though it was loaded on conductive CNT supports. The exact mechanism underlying the enhanced electrocatalysis of GOCNT–Pt nanocomposites has not been well-understood so far, although Pt Nanos have been well established as super catalysts to exert high electrocatalysis effects on H_2O_2 or glucose.[41,42] Nevertheless, it is likely related to some synergistic factors involving the unique structures of the carbon supports of CNTs and GO nanosheets, and improved spatial distribution and electron-transferring ability of Pt Nanos on GOCNTs.[43–46] Significantly, it confirms that metal-support interactions can largely affect the activity of metal nanocatalysts so supported. Since GO-dispersed CNTs have a better organized graphitic structure, which is more ordered than that of carbon black, the Pt–CNT interactions can change the crystal structures of Pt nanocatalysts on GOCNTs towards greatly enhanced electrocatalysis activity.[44] On the one hand, the Pt products formed on CNTs are defined as "interconnected" Pt Nanos, which are more active than original Pt Nanos.[45] On the other hand, upon deposition, the finely dispersed Pt Nanos can bind to carbon supports *via* bonding with ester and carbonyl O atoms in the form of COO(Pt) and C(=O)CO(Pt), and the Pt–CNT distribution density and surface structures can play a key role in improving their electrocatalysis.[46] Also, carbon supports with delocalized π electrons of graphite sheets might help to improve Pt surface properties and promote electron shuttling to and from its catalysis active sites as aforementioned.

2.4. Preliminary catalysis-based sensing applications of GOCNT–Pt nanocomposites

To further explore the application feasibility of the new enzyme mimics, a H_2O_2 sensor was fabricated with the GOCNT–Pt nanocatalysts for the direct electrochemical H_2O_2 sensing. Fig. 5A manifests a current–time response curve recorded at an applied potential of −0.2 V by successive additions of H_2O_2. The current responses reached a steady-state signal within ~5 s. The steady-state calibration curve of H_2O_2 responses for the amperometric enzyme sensor is shown in Fig. 5B. Accordingly, a linear range from 2.5×10^{-6} to 1.0×10^{-2} M H_2O_2 was achieved for the direct H_2O_2 detection. Moreover, the interferential experiments of the H_2O_2 sensor were conducted with the results shown in Table S2, ESI.†

It was found that most of co-existing common molecules or ions might show no interference for the determination of H_2O_2. But obvious interferences were observed for glucose, ascorbic acid and S^{2-} with considerably high concentrations, presumably originating from those interferents that might inhibit the catalysis activity of the Pt catalysts or take part in the redox reactions. Also, 2.0 mM H_2O_2 was measured by the electrode once a week for 10 weeks, and a relative standard deviation of 6.2% was obtained, showing a favorable reproducibility of the analysis. In addition, the GOCNT–Pt electrode could work well at different temperatures such as 40 °C, 60 °C and 90 °C, as well as pH values of 1.0 to 14 (data not shown). The data prove that GOCNT–Pt nanocomposites at the electrodes can retain high catalysis stability over extreme operational environments.

Moreover, the coupling of natural peroxidases as amplifying biocatalytic labels is a common paradigm in developing biosensing devices. In this work, GOCNT–Pt catalysts were applied as the enzyme labels for secondary antibodies for the electrochemical immunoassay of immunoglobulin G (IgG) by static amperometric measurements (Fig. 6). Fig. 6A shows the results of electrochemical IgG immunoassays, with bovine serum albumin (BSA) serving as a control. One can note that the sandwich immunoassays can illustrate static currents proportional to IgGs with concentrations ranging from 5.0 to 625 μg mL^{-1}. Moreover, high detection specificity of the sandwich IgG immunoassay is evident by the significantly low response to BSA, as also reflected in the real-time static amperometric responses (Fig. 6B). Therefore, the GOCNT–Pt nanocatalysts can

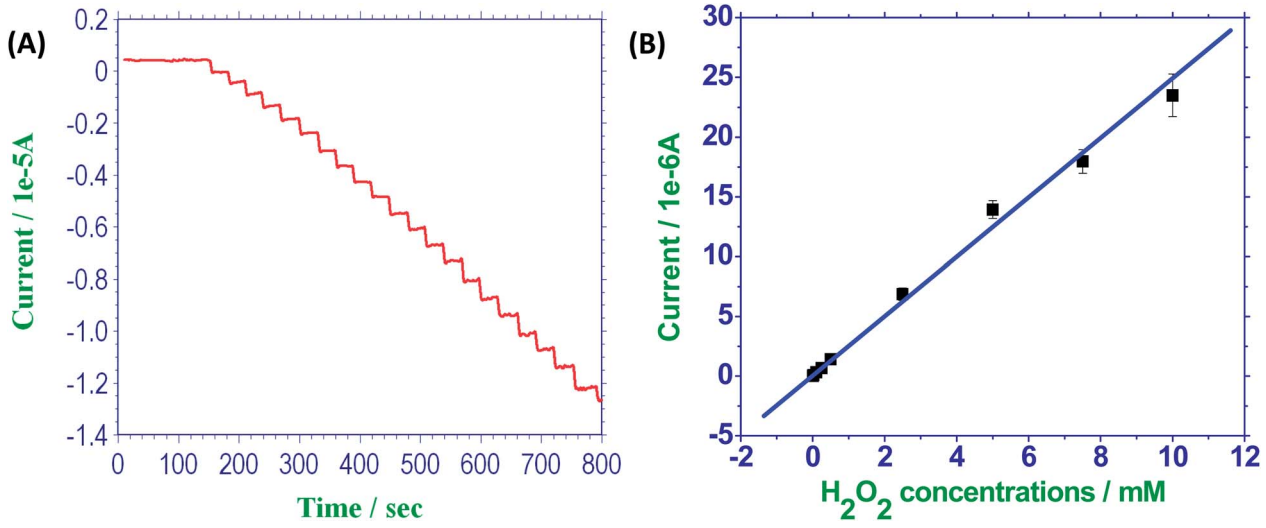

Fig. 5 (A) Typical current–time responses of the GOCNT–Pt electrode to H_2O_2 successively added with a step of 0.2 mM at an applied potential of −0.2 V. (B) The steady-state calibration curve of amperometric responses of the GOCNT–Pt sensor to H_2O_2 with different concentrations in (A).

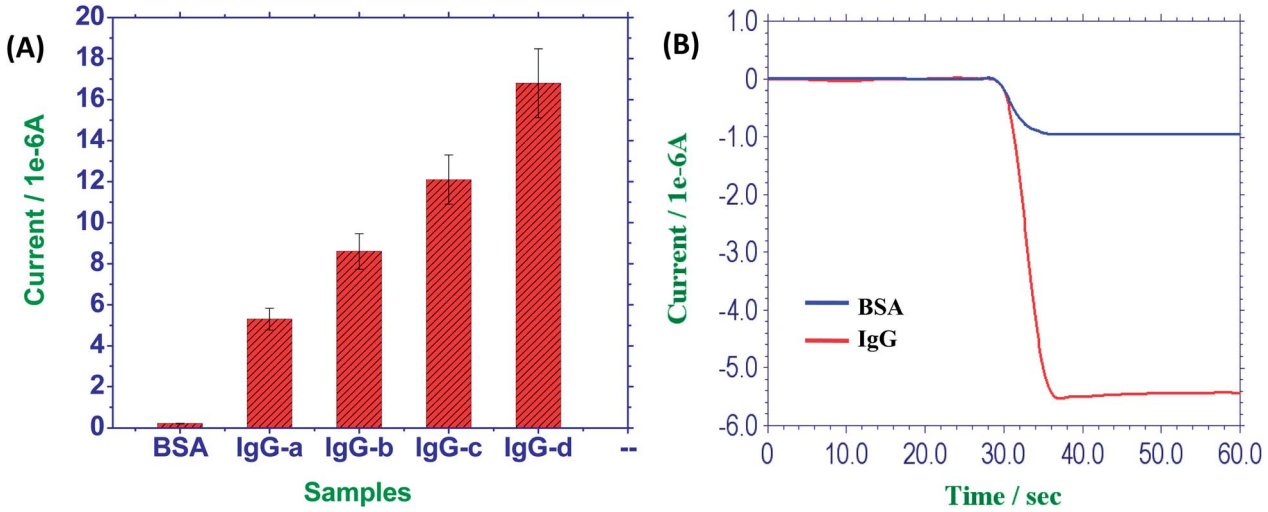

Fig. 6 (A) Electrochemical sandwich immunoassays for IgGs of different concentrations using GOCNT–Pt labeled IgGAbs, taking 1.0 mg mL^{-1} BSA as a control (IgG-a to d corresponding to 5.0, 25, 125 and 625 μg mL^{-1}). (B) Comparison of real-time static amperometric responses between 5.0 μg mL^{-1} IgG and 1.0 mg mL^{-1} BSA when adding 8.8 mM H_2O_2.

be potentially employed as new catalytic labels of recognition molecules for wide enzyme-based electrochemical and optical sensing assays.

3. Experimental section

3.1. Materials and reagents

Graphene oxide (GO) nanosheets were obtained from Graphene Supermarket (USA). Multiwalled carbon nanotubes (CNTs) with ~95% purity were obtained from NanoLab (Brighton, MA). Mouse IgGs, anti-mouse IgG antibodies (IgGAbs), IgGAbs labeled with horseradish peroxidase (HRP), bovine serum albumin (BSA), Nafion (5.0%), ethyl(dimethylaminopropyl) carbodiimide (EDC), *N*-hydroxysuccinimide (NHS), HRP (EC 1.11.1.7), hexachloroplatinic acid, DL-dithiothreitol (DDT), gold nanoparticles (10 nm in diameter), and peroxidase substrate solution were the products of Sigma-Aldrich, including organic substrates of 3,3′,5,5′-tetramethylbenzidine (TMB), 3,3′-diaminobenzidine (DAB), *p*-phenylenediamine (PPD), *p*-aminophenol (PAP), and hydroquinone (HQ). Other reagents were of analytical reagent grade.

3.2. Synthesis of GOCNT–Pt nanocomposites

The GO-dispersed CNTs (GOCNTs) were prepared with the mass ratio of GO nanosheets to CNTs of 1 : 10. An appropriate amount of CNTs was ultra-sonicated in deionized water for 30 min, and then GO solution was added into the CNT solution to be further sonicated until a visually homogeneous dispersion was formed. The resulting mixture was sonicated for 16 h (60 s on and 5 s off cycles) and then centrifuged and washed to form GOCNTs.

Furthermore, GOCNT–Pt nanocomposites were synthesized with the impregnation method using H_2 as the reducing agent.

Typically, an appropriate amount of hexachloroplatinic acid was dissolved in acetone. GOCNTs with the required dosage were dispersed in an appropriate amount of Pt precursor solution under mild stirring. The mixture was then incubated in the oven overnight at 100 °C. The mixture was further treated under a H_2 environment for 2 h at 300 °C with a ramping rate of 0.5 °C min^{-1}. The GOCNT–Pt catalysts (20 wt% Pt) so obtained were collected and further were re-dispersed in GO nanocolloids in the same ratio as above. Moreover, for the purpose of comparison, pre-acidized GO, and CNT powders were treated by the same way under the H_2 environment for 2 h at 300 °C, so did the CNT–Pt and GO–Pt nanocomposites. TEM measurements (Hitachi H-7000, Japan) were conducted for different materials dispersed in 2-propanol. Moreover, the as-prepared GOCNT–Pt nanocomposites were diluted to 1.0 mg mL^{-1} in 2-propanol containing 0.25% Nafion to be stored at 4 °C.

3.3. Evaluation of dispersion stabilities of GOCNT–Pt and CNT–Pt nanocomposites

The dispersion stabilities of GOCNT–Pt and CNT–Pt nanocomposites were investigated comparably by using dynamic light scattering (DLS) with a Zetasizer Nano ZS (Malvern Instruments, UK) setup equipped with a helium–neon laser (λ = 632.8 nm, 4 mW) and a thermoelectric temperature controller. The samples were diluted to a certain concentration and sonicated for 1 h. DLS measurements were then performed at a 90° scattering angle in a 3 × 3 mm quartz cuvette, in which 18 runs of 10 seconds were carried out for each of samples to obtain the averaged nanotube sizes (hydrodynamic diameters). Moreover, the time-dependent dispersion of the GOCNT–Pt and CNT–Pt suspensions was monitored by DLS as well as UV/vis measurements (UV-3600 spectrophotometer, Shimadzu, Japan). The samples were well dispersed and placed over time. The sample supernatants were carefully taken out at different time intervals (2.0, 5.0, 10, 24, 48, 72, 120, and 192 h) for DLS and UV/vis measurements separately. The DLS intensities of the

meaningful size range of nanotubes and optical absorbance values at 250 nm were recorded over time.

3.4. Preparation of CNT–HRP and GOCNT–Pt-labeled IgGAb conjugates

The as-prepared CNTs and GOCNT–Pt powders were separately dispersed to 1.0 mg mL^{-1} in PBS buffer (pH 7.2) containing 0.50% Triton X-100, 100 mM EDC, and 80 mM NHS to be chemically activated for 1 h, and then washed twice. To prepare the CNT–HRP conjugate, the CNT suspensions were mixed with 20 mg mL^{-1} HRP to be incubated overnight at 4 °C. Then, the mixture was centrifuged and washed twice with PBS buffer. Subsequently, the resulting CNT–HRP conjugate was diluted to 1.0 mg mL^{-1} CNTs to be stored at 4 °C. Following the same procedure, the GOCNT–Pt-labeled IgGAb conjugates were prepared except for using 2.0 mg mL^{-1} secondary IgGAbs.

3.5. Colorimetric catalysis tests

Colorimetric investigation of peroxidase-like activities of GOCNT–Pt nanocomposites was performed using the commercially-available TMB-H_2O_2 substrate, when compared to CNT, GO, Pt Nano, CNT–Pt, and GO–Pt nanocomposites of certain concentrations indicated. Moreover, the catalytic oxidization of some organic substrates including TMB, DAB, PPD, PAP and HQ was conducted by using GOCNT–Pt nanocomposites. Each of the organic substrates (1.0 mM) was mixed with 0.05 mg mL^{-1} GOCNT–Pt nanocomposites and 4.0 mM H_2O_2 in N_2-saturated PBS buffer to be reacted for 15 min to produce different colors.

The colorimetric detections for H_2O_2 with different concentrations (1.0×10^{-7} to 1.0×10^{-2} M) were conducted in N_2-saturated PBS buffer in the presence of 1.0 mM TMB separately using 0.05 mg mL^{-1} GOCNT–Pt nanocomposites, 0.01 mg mL^{-1} Pt Nanos, and 0.01 mg mL^{-1} HRP. Moreover, the dynamics parameters (*i.e.*, K_m and V_{max}) of GOCNT–Pt, CNT–Pt, and GO–Pt nanocomposites were measured accordingly to plot Michaelis–Menten curves with different concentrations of H_2O_2 and TMB.

3.6. Electrochemical H_2O_2 analysis

Electrochemical voltammetric measurements for the electrocatalytic responses of the GOCNT–Pt modified electrodes to H_2O_2 were performed in the presence and absence of TMB using an electrochemical analyzer CHI 760 (CH Instruments, Austin, TX), which is connected to a personal computer. A three-electrode configuration (CH Instruments) consisting of a glass carbon (GC) working electrode, an Ag/AgCl reference electrode and a platinum counter electrode was employed. Herein, the GC working electrodes were polished and further coated with GOCNT–Pt nanocomposites, compared with those modified separately with CNTs, Pt Nanos, GO–Pt, and CNT–Pt nanocomposites or CNT-loaded HRP conjugates. In brief, each of the stock nanomaterials (except for Pt Nano) was first diluted to 1.0 mg mL^{-1} in PBS buffer containing 0.25% Nafion. After being dispersed by sonication, 5.0 μL of each of the nanomaterial suspensions was dropped separately onto the polished GCE electrodes to be incubated overnight at 4 °C. Following that, 5.0 μL of 0.05% Nafion was added onto each of the electrodes and left for 1 h at room temperature. The preparation of the Pt Nano electrode was conducted accordingly but for using 0.2 mg mL^{-1} Pt Nano. Subsequently, the as-prepared electrodes were used separately to detect 2.0 mM H_2O_2 in a 5 mL voltammetric cell with N_2-saturated PBS buffer in the presence and absence of 0.4 mM TMB, scanning from −0.6 to +0.4 V at a scan rate of 0.10 V s^{-1}. Moreover, the current–time responses of the GOCNT–Pt electrode toward successive additions of 0.2 mM H_2O_2 were obtained at an applied potential of −0.2 V. All potentials were referred to the Ag/AgCl reference electrode.

3.7. Electrochemical immunoassays

Electrochemical sandwich immunoassays for IgGs with different concentrations were conducted on gold electrodes (2 mm diameter, CH Instruments) using GOCNT–Pt catalysts and secondary IgGAbs. Here, the gold electrodes were first dipped into 2.0 mg mL^{-1} DDT for 2 h at room temperature and then washed twice with PBS buffer. Furthermore, 5.0 μL of gold nanoparticles were dropped onto it overnight, and then washed twice. Following that, 5.0 μL IgGAbs (1.0 mg mL^{-1}) was injected onto the electrodes to be incubated overnight at 4 °C, followed by two washings. After being blocked by 10 mg mL^{-1} BSA, each 5.0 μL of IgG samples was introduced onto the electrodes to be incubated for 1 h at 37 °C and then washed twice. Following that, 5 μL of GOCNT–Pt-labeled IgGAbs was introduced onto the electrodes to recognize the captured IgGs in the same way. Subsequently, static amperometric measurements for the resulting immunosensors were performed at an applied potential of −0.2 V in PBS buffer.

4. Conclusions

Platinum (Pt) nanocatalysts supported on carbon nanotubes (CNTs) have been well established to present high electrocatalysis and power density. However, few investigations have been conducted systematically on their peroxidase-like catalysis activities especially their catalysis performances in water, which could be challenged by the poor aqueous dispersion of hydrophobic carbon supports and the undesirable spatial distribution of Pt nanocatalysts loaded. In this work, hydrophobic CNTs have been well dispersed in GO nanocolloids to achieve a stable aqueous suspension as conductive supports for loading Pt nanocatalysts. The resulting GOCNT–Pt nanocomposites were re-dispersed in GO nanocolloids so as to obtain high aqueous dispersion stability and good spatial distribution density of Pt nanocatalysts. Importantly, colorimetric and electrochemical investigations indicate that the developed inorganic nanocatalysts could display much higher peroxidase-like catalysis and electrocatalysis activities than some inorganic nanocatalysts commonly used. Also, the so prepared enzyme mimic could exhibit aqueous catalysis performances comparable to protein peroxidase; yet, they may have some advantages over natural enzymes in terms of higher catalysis efficiency, electron transfer, aqueous stability, environmental robustness, and cost effectiveness. They could catalyze the H_2O_2-induced oxidation

of typical organic substrates, indicating the applications for catalytic degradation of toxic organic species (*i.e.*, phenols) so as to reduce their toxicity in the environment. Moreover, electrochemical measurement results demonstrate that the GOCNT–Pt nanocomposites could present stronger electrocatalysis than natural enzymes (*i.e.*, HRP) in the reduction of H_2O_2 as well as the oxidation of organic substrates like TMB. In addition, sandwich-based immunoassays have been successfully performed for model proteins of IgGs using GOCNT–Pt catalysts as the enzymatic tags, indicating that they may promise very attractive applications for enzyme-based aqueous assays and biosensors, including the catalysis reactions that are mostly carried out in water. Although more efforts will be necessarily made to better understand at the molecular scale the catalysis mechanism underlying for the carbon-supported Pt nanocatalysts, such a preparation method for inorganic nanocatalysts combining noble metal nanocatalysts and well-dispersed conductive carbon supports may open a new door toward the design of different "artificial enzymes".

Acknowledgements

This work is supported by the National Institutes of Health Counter ACT Program by the National Institute of Neurological Disorders and Stroke (award # NS058161-01), the National Natural Science Foundation of China (no. 21375075), and the Taishan Scholar Foundation of Shandong Province, P. R. China. The contents of this publication are solely the responsibility of the authors and do not necessarily represent the official views of the Federal Government. PNNL is operated by Battelle for DOE under Contract DE-AC05-76RL01830.

Notes and references

1 P. Nannipieri and J. M. Bollag, *J. Environ. Qual.*, 1991, **20**, 510–517.
2 H. Park and Y. K. Choung, *Hum. Ecol. Risk Assess.*, 2007, **13**, 1147–1155.
3 A. Mueller, *Mini-Rev. Med. Chem.*, 2005, **5**, 231–239.
4 J. Wang, *Analyst*, 2005, **130**, 421–426.
5 A. J. Kirby, *Angew. Chem., Int. Ed.*, 1994, **33**, 551–553.
6 V. Nanda and R. L. Koder, *Nat. Chem.*, 2010, **2**, 15–24.
7 Z. Genfa and P. K. Dasgupta, *Anal. Chem.*, 1992, **64**, 517–522.
8 L. Fruk and C. M. Niemeyer, *Angew. Chem., Int. Ed.*, 2005, **44**, 2603–2606.
9 R. Breslow, X. J. Zhang and Y. Huang, *J. Am. Chem. Soc.*, 1997, **119**, 4535–4536.
10 W. C. Ellis, C. T. Tran, M. A. Denardo, A. Fischer, A. D. Ryabov and T. J. Collins, *J. Am. Chem. Soc.*, 2009, **131**, 18052–18053.
11 L. Z. Gao, J. Zhuang, L. Nie, J. B. Zhang, Y. Zhang, N. Gu, T. H. Wang, J. Feng, D. L. Yang, S. Perrett and X. Yan, *Nat. Nanotechnol.*, 2007, **2**, 577–583.
12 Y. J. Song, K. G. Qu, C. Zhao, J. S. Ren and X. G. Qu, *Adv. Mater.*, 2010, **22**, 1–5.
13 T. Hamasaki, T. Kashiwagi, T. Imada, N. Nakamichi, S. Aramaki, K. Toh, S. Morisawa, H. Shimakoshi, Y. Hisaeda and S. Shirahata, *Langmuir*, 2008, **24**, 7354–7364.
14 M. Ma, Y. Zhang and N. Gu, *Colloids Surf., A*, 2011, **373**, 6–10.
15 R. H. Baughman, A. A. Zakhidov and W. A. de Heer, *Science*, 2002, **297**, 787–792.
16 M. C. Hersam, *Nat. Nanotechnol.*, 2008, **3**, 387–394.
17 W. Z. Li, C. H. Liang, W. J. Zhou, J. S. Qiu, Z. H. Zhou, G. Q. Sun and Q. Xin, *J. Phys. Chem. B*, 2003, **107**, 6292–6299.
18 G. Girishkumar, M. Rettker, R. Underhile, D. Binz, K. Vinodgopal, P. McGinn and P. Kamat, *Langmuir*, 2005, **21**, 8487–8494.
19 M. Kaempgen, M. Lebert, N. Nicoloso and S. Roth, *Appl. Phys. Lett.*, 2008, **92**, 094103.
20 J. Wang and Y. H. Lin, *TrAC, Trends Anal. Chem.*, 2008, **27**, 619–626.
21 M. Trojanowicz, *TrAC, Trends Anal. Chem.*, 2006, **25**, 480–489.
22 J. Yan, H. J. Zhou, P. Yu, L. Su and L. Q. Mao, *Adv. Mater.*, 2008, **20**, 2899–2906.
23 G. D. Liu and Y. H. Lin, *Anal. Chem.*, 2006, **78**, 835–843.
24 C. Wang, M. Waje, X. Wang, J. M. Tang, R. C. Haddon and Y. S. Yan, *Nano Lett.*, 2004, **4**, 345–348.
25 S. Hrapovic, Y. L. Liu, K. B. Male and J. H. T. Luong, *Anal. Chem.*, 2004, **76**, 1083–1088.
26 M. H. Yang, Y. Yang, H. F. Yang, G. L. Shen and R. Q. Yu, *Biomaterials*, 2006, **27**, 246–255.
27 J. N. Me, S. Y. Wang, L. Aryasomayajula and V. K. Varadan, *J. Mater. Res.*, 2008, **23**, 1457–1465.
28 M. S. Saha and A. Kundu, *J. Power Sources*, 2010, **195**, 6255–6261.
29 J. Wang, M. Musameh and Y. H. Lin, *J. Am. Chem. Soc.*, 2003, **125**, 2408–2409.
30 X. L. Li, X. R. Wang, L. Zhang, S. Lee and H. J. Dai, *Science*, 2008, **319**, 1229–1232.
31 L. J. Cote, J. Kim, V. C. Tung, J. Luo, F. Kim and J. Huang, *Pure Appl. Chem.*, 2011, **83**, 95–110.
32 J. Ma, L. Zhou, C. Li, J. H. Yang, T. Meng, H. M. Zhou, M. X. Yang, F. Yu and J. H. Chen, *J. Power Sources*, 2014, **247**, 999–1004.
33 L. L. Tian, M. J. Meziani, F. S. Lu, C. Kong, Y. L. Cao, T. J. Thorne and Y. P. Sun, *ACS Appl. Mater. Interfaces*, 2010, **2**, 3217–3222.
34 S. C. Sahu, A. K. Samantara, B. Satpati, S. Bhattacharjee and B. K. Jena, *Nanoscale*, 2013, **5**, 11265–11274.
35 B. P. Vinayan, R. Nagar and S. Ramaprabhu, *J. Mater. Chem.*, 2012, **22**, 25325–25334.
36 S. H. Joo, S. J. Choi, I. Oh, J. Kwak, Z. Liu, O. Terasaki and R. Ryoo, *Nature*, 2001, **412**, 169–172.
37 H. Tang, J. H. Chen, Z. P. Huang, D. Z. Wang, Z. F. Ren, L. H. Nie, Y. F. Kuang and S. Z. Yao, *Carbon*, 2004, **42**, 191–197.
38 J. N. Wang, Y. Z. Zhao and J. J. Niu, *J. Mater. Chem.*, 2007, **17**, 2251–2256.
39 M. Ma, Y. Zhang and N. Gu, *Colloids Surf., A*, 2011, **373**, 6–10.
40 A. Harriman, G. R. Millward, P. Neta, M. C. Richoux and J. M. Thomas, *J. Phys. Chem.*, 1988, **92**, 1286–1290.

41 T. Y. You, O. Niwa, M. Tomita and S. Hirono, *Anal. Chem.*, 2003, **75**, 2080–2085.
42 J. H. Yuan, K. Wang and X. H. Xia, *Adv. Funct. Mater.*, 2005, **15**, 803–809.
43 Y. Y. Mu, H. P. Liang, J. S. Hu, L. Jiang and L. J. Wan, *J. Phys. Chem. B*, 2005, **109**, 22212–22216.
44 L. Li and Y. C. Xing, *J. Phys. Chem. C*, 2007, **111**, 2803–2808.
45 S. Y. Wang, S. P. Jiang, T. J. White, J. Guo and X. Wang, *J. Phys. Chem. C*, 2009, **113**, 18935–18945.
46 R. V. Hull, L. Li, Y. C. Xing and C. C. Chusuei, *Chem. Mater.*, 2006, **18**, 1780–1788.